Journal of Applied Polymer Science

Biodegradable nanocomposites based on starch/polycaprolactone/compatibilizer ternary blends reinforced with natural and organo-modified montmorillonite

M. P. Guarás, V. A. Alvarez, L. N. Ludueña
Research Institute of Material Science and Technology (INTEMA), Composite Materials Group (CoMP) Engineering Faculty, National University of Mar Del Plata, Juan B. Justo 4302, B7608FDQ, Mar Del Plata, Argentina
Correspondence to: L. N. Ludueña (E-mail: luduenaunmdp@gmail.com)

ABSTRACT: In this article, biodegradable polymer/clay nanocomposites were prepared. The matrices used were based on blends of Polycaprolactone (PCL) and Anhydride-Functional Polycaprolactone (PCL-gMA) with Thermoplastic Starch (TPS). Nanocomposites films based on PCL/TPS and PCL/PCL-g-MA/TPS blends reinforced with 1 and 3 wt % of natural montmorillonite and two organo-modified ones were prepared by melt intercalation followed by compression molding. The study was designed focusing on packaging applications. Grafting maleic anhydride onto PCL was efficient to improve PCL/TPS compatibility but did not modify matrix/nanoclay interaction. Matrix compatibilization and nanoclays increased the Youngs modulus and slightly decreased the maximum stress of the TPS/PCL matrix. Nanoclay functionalization improved nanoclay dispersion in the blends but it was not reflected in mechanical properties improvements. The water adsorption of the compatibilized matrix was reduced after clay incorporation. A slight decrease in the biodegradation rate was observed with the addition of nanoclay. © 2016 Wiley Periodicals, Inc. J. Appl. Polym. Sci. **2016**, *133*, 44163.

KEYWORDS: biopolymers and renewable polymers; blends; clay; compatibilization; packaging

Received 12 April 2016; accepted 7 July 2016
DOI: 10.1002/app.44163

INTRODUCTION

Polymeric materials have a wide range of distinctive properties: they are malleable, flexible, and capable of being molded to complex shapes. They are lightweight, which implies easiness in handling and cost optimization. The increasing demand on these materials in the last decades has caused many environmental problems associated with their disposal. Although recycling may be a solution in some cases, many plastics cannot be recycled, especially when they are used in applications involving food packaging, hygiene, or some medical devices. For these reasons, biodegradable plastics are becoming an attractive alternative to conventional polymers.

Polycaprolactone (PCL) is synthetic aliphatic polyester that can be completely biodegraded by enzymatic activity. Its main advantages are its good processability and high elongation at break, but it has low rigidity and tensile strength, and its cost is too high to be used for packaging applications. A possible solution is to blend PCL with less-expensive biodegradable polymers such as starch.[1]

Starch is a natural biodegradable polymer existing in many vegetables as the main energy source. It is inexpensive, but its complex granular structure makes it difficult to process by conventional methods, so it needs to be modified with the addition of a plasticizer applying heat and shear forces. This leads to thermoplastic starch (TPS), which can be processed as a conventional thermoplastic material.[2]

TPS has been blended with PCL without much success because of poor interfacial compatibility, and the blends have shown an increased water absorption tendency because of the hydrophilic nature of starch. However, the addition of a compatibilizer, like maleic anhydride-grafted-polycaprolactone (PCL-gMA), enhances the compatibility, increasing mechanical properties and lowering the water permeability of the blends.[3,4]

Nevertheless, the improvement in those properties is not enough to be competitive with many traditional plastics. The addition of nanofillers to polymers has been showed to be an effective way of further enhancing mechanical and barrier properties. Nanoclay has been widely studied as they are an easily available and low-cost alternative compared to other nanofillers.[5] Starch/nanoclay and PCL/nanoclay blends have been studied, achieving better mechanical (higher Youngs modulus and tensile strength) and barrier properties,[6–11] but there are not many works combining these materials.

In a previous work,[6] we studied the effect of TPS formulation, PCL/TPS ratio, and PCL-gMA content on the morphology,

Table I. Characteristics of the Used Nanoclays

Clay	Organic modifier[a]	*OC* (wt %)[b]	d_{001}^{final} (Å)	$M_{24\ h\text{-}90\%\ RH}$ (%)
Montmorillonite (CNa^+)	—	0	11.9	12.99
Cloisite 30B (C30B)	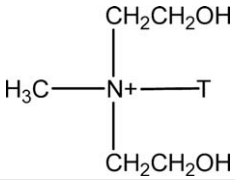	28	18.8	3.98
Cloisite 20A (C20A)	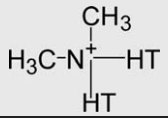	40	26.7	3.22

[a] HT: hydrogenated tallow (65% C18; 30% C16; 5% C14).
[b] *OC* = Organic content calculated by TGA from the mass loss between 150 °C and 500 °C.

thermal, mechanical and barrier properties, and biodegradation in soil of PCL/PCL-gMA/TPS ternary blends. Phase separation was observed in all samples by scanning electron microscopy (SEM). It was shown that the size of the TPS phase was reduced and its dispersion and distribution in the PCL phase was improved after compatibilization with PCL-gMA. The optimal morphology, mechanical, and barrier properties were obtained with the TPS prepared with 25 wt % of plasticizer and blends containing 25 wt % of TPS, 70 wt % of PCL, and 5 wt % of PCL-gMA.

The aim of this article was to improve the performance of the PCL/PCL-gMA/TPS blends prepared with the optimized formulation[6] by nanoclays incorporation in order to obtain biodegradable nanocomposites for packaging applications. Clay dispersion degree and clay content are the typical parameters used in the bibliography to correlate them with the final properties of polymer/clay nanocomposites. In this article, we focus on additional parameters acting simultaneously governing the final performance of the nanocomposites.

EXPERIMENTAL

Materials

Cassava starch was used in powder form. The plasticizer used was ethylene glycol (EG, JT Baker). Stearic acid was used (SA Shuchardt Merck OHG) as a lubricant for processing.

Polycaprolactone, having a molar mass of 80,000 g/mol was supplied by Aldrich Chemistry. Maleic anhydride (MA), Carlo Erba Reagents product, was used to make the compatibilizer. Benzoyl peroxide (BP) from Aldrich Chemistry was used as initiator of the grafting reaction.

Three Cloisite® commercial clays (Cloisite Na+ is a natural montmorillonite; Cloisite 20A and Cloisite 30B are natural montmorillonites modified with quaternary ammonium salts) purchased from Southern Clay Products, USA, were used as nanofillers. They were used as received. The characteristics of the clays are shown in Table I.

Preparation of TPS

Native starch and plasticizer (ethylene glycol) were premixed in a beaker. Before mixing, native starch was dried for 48 h at 45 °C in vacuum oven. The composition of the mixture was 75/25 wt % for native starch/plasticizer, respectively. Then, TPS was prepared in a Brabender type mixer at 120 °C and 60 rpm for 6 min. A small amount of stearic acid (0.5 wt %) was added as a processing agent. TPS was named TPS. Mixing conditions and TPS composition were optimized in a previous work.[6]

Preparation of the Compatibilizer

The compatibilizer was prepared by blending 95/4.5/0.5 wt % of PCL/MA/BP in a Brabender Type mixer at 110 °C and 60 rpm for 7 min. The compatibilizer was called PCL-gMA. The composition was based on a previous work.[6]

Preparation of the PCL/PCL-gMA/TPS Blends Reinforced with Nanoclays

The different contents of PCL, PCL-gMA, and TPS were fed simultaneously into the Brabender type mixer at 110 °C and 60 rpm for 6 min. Before feeding, the components were dried for 48 h at 45 °C in vacuum oven. The optimal compositions of these blends were found in a previous work.[5] In the case of the compatibilized blends, the PCL/PCL-gMA/TPS composition was 70/5/25 wt %, respectively, while the composition of the uncompatibilized ones was 75/0/25 wt % for PCL/PCL-gMA/TPS, respectively. Then, 1 and 3 wt % of each nanoclay was fed to these matrices. Before feeding nanoclays were dried for 48 h at 90 °C. Nanoclays were fed at the third minute of the blending process, maintaining a total mixing time of 6 min in all cases.

Then, films of 0.7 × 150 × 200 mm^3 were obtained by compression molding: 10 min at 120 °C and 0 kg/cm^2, 10 min at 120 °C and 50 kg/cm^2, and finally mold cooling with water up to 30 °C. The films were identified by three numbers indicating the composition, i.e., 70/5/25/1C20A, where the first three numbers corresponds to the composition of the matrices, and the last code to the wt % and type of nanoclay.

Characterization of Blends

Differential Scanning Calorimetry. was carried out by using a Q2000 TA Instrument. An empty pan of aluminum was used as reference. About 8 mg of the samples were weighed accurately into aluminum pans and sealed hermetically. The samples were cooled down to −80 °C, and then heated to 250 °C at a scan

rate of 10 °C/min. Finally they were cooled down to room temperature. Four samples of each material were tested for statistical analysis.

Thermogravimetric Tests. were carried out with a TA Instruments TGA HI-Res^{TM}500. Samples were heated at a constant rate of 10 °C/min from room temperature to 700 °C, under nitrogen atmosphere. TGA curves were used to calculate the TPS and PCL content of blends. Derivative thermogravimetric analysis (DTGA) was performed in order to identify the temperatures for the maximum thermal degradation rates of the components. Four samples of each material were tested for statistical analysis.

Tensile Tests. were performed on an INSTRON 4467 machine using a load cell of 100 N and operating at a constant crosshead speed of 1 mm/min. Samples were prepared according to the ASTM D882-91 standard. Prior to mechanical measurements, the samples were conditioned at 65% relative humidity for 48 h at room temperature. Five samples of each material were tested for statistical analysis.

X-ray Diffraction (XRD). was performed in an Analytical Expert Instrument (K∞Cu = 1.54 Å) from 2θ = 3° to 60° (2°/min) at room temperature. The generator voltage was 40 kV and the current was 40 mA. The interlayer spacing of clays was calculated before and after mixing by means of the **Braggs Law**. The values were named as d_{001}.

Water Absorption Experiments. were performed according to the ASTM D 5229 standard. Prior to the water absorption measurements, the samples were dried in a vacuum oven at 30–35 °C for 48 h. The samples were conditioned in hermetic containers at room temperature with 90% relative humidity, using a solution of glycerin and water. The amount of water absorbed by the samples was determined by weighing them periodically, until a constant weight was attained. The water uptake [$W(\%)$] was given by the following equation:

$$W(\%) = \frac{M_t - M_0}{M_0} \times 100\% \quad (1)$$

where M_t is the weight at time t and M_0 the initial weight.

Equilibrium water absorption (W_{eq}) was calculated from the maximum absorbed water of the plots W as a function of $t^{1/2}$. Three samples of each material were tested for statistical analysis.

Biodegradability of the Samples. was studied by evaluating weight loss of blends as a function of time in a soil environment. Samples of 15 × 15 × 0.7 mm^3 were weighed and then buried in boxes with soil. Natural microflora present in soil (Pinocha type) was used as the biodegrading medium. Soil was maintained at approximately 50% moisture in weight and samples were buried at a depth of 15 cm. The samples were dried before burying them in a vacuum oven for 48 h at 35 °C. At these conditions constant weight was attained. Then, once unearthed, the samples were weighted to measure the water absorption and after that were dried in a vacuum oven at 35 °C for 48 h to measure the weight loss. Three samples of each material were tested for statistical analysis.

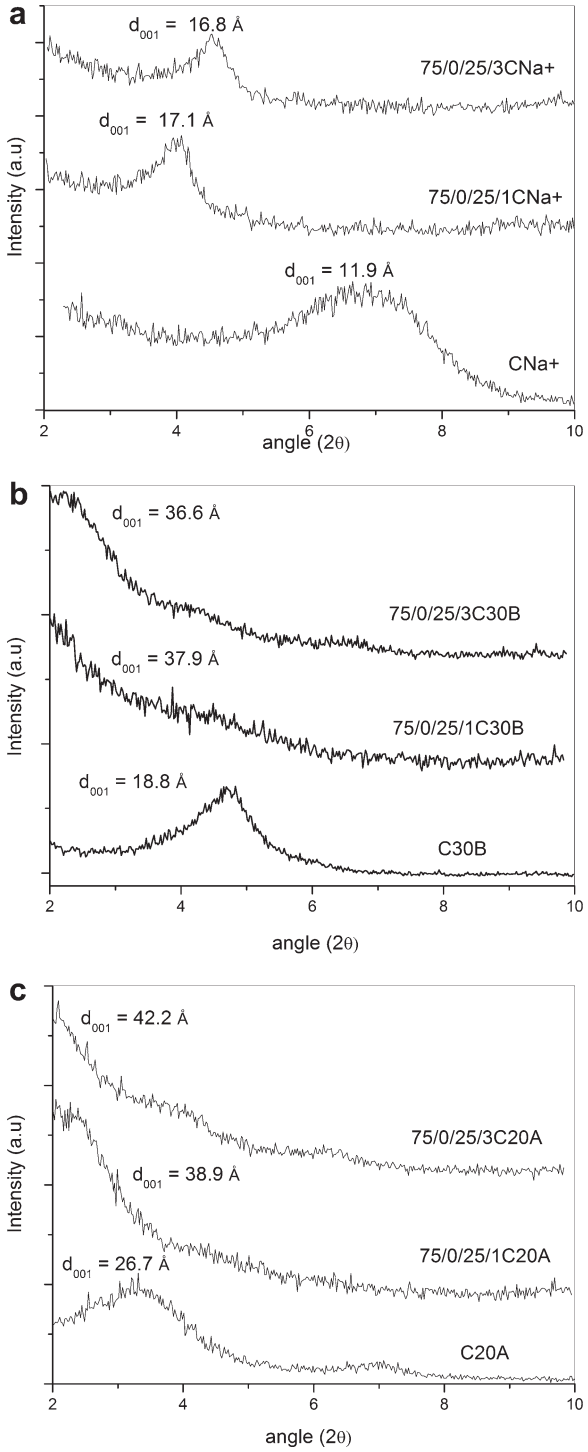

Figure 1. XRD spectra of clay alone and nanocomposites based on PCL/TPS reinforced with: (a) CNa+, (b) C30B, and (c) C20A.

RESULTS AND DISCUSSION

Morphology (XRD)

Figure 1(a–c) show the XRD spectra of clay and nanocomposites based on the uncompatibilized matrix. Similar curves were obtained for the compatibilized matrix but were not shown for the sake of simplicity.

Table II. Interlayer Spacing of the Neat Nanoclays and Nanocomposites

Sample	Δd_{001} (Å)	Δd_{001}(%)	Sample	d_{001}^{final} (Å)	Δd_{001} (%)	Sample	d_{001}^{final} (Å)	Δd_{001} (%)
CNa+	11.9	—	C30B	18.8	—	C20A	26.7	—
75/0/25/1CNa+	17.1	44	75/0/25/1C30B	37.9	102	70/0/25/1C20A	38.9	47
75/0/25/3CNa+	16.8	29	75/0/25/3C30B	36.6	95	70/0/25/3C20A	42.2	58
70/5/25/1CNa+	17.0	43	70/5/25/1C30B	40.3	114	70/5/25/1C20A	39.2	47
70/5/25/3CNa+	17.0	43	70/5/25/3C30B	40.7	116	70/5/25/3C20A	41.8	57

The interlaminar space of the neat nanoclays ($d_{001}^{initial}$ reported in Table I) and inside the nanocomposites (d_{001}^{final}) were calculated from XRD spectra by means of the **Braggs Law**. The morphology of the nanocomposites was analyzed by means of the interlayer spacing of the clay inside the nanocomposites (d_{001}^{final}) and the increment in the interlayer distance ($\Delta d_{001} = ((d_{001}^{final} - d_{001}^{initial})/d_{001}^{initial})100$). Table II shows the d_{001}^{final} and Δd_{001} values of the nanocomposites.

It is expected that as $d_{001}^{initial}$ increases, polymer chains have more space to intercalate. How many polymer chains intercalate between the silicate layers will depend on the silicate surface/polymer chemical compatibility, assuming nanocomposites prepared by identical conditions without thermal degradation of nanoclay organo-modifiers during processing. Thermal degradation of the organo-modifiers was studied in a previous work, confirming that the processing conditions used in this work do not degrade those of C30B and C20A.[11] The interlaminar space of the nanoclays inside the nanocomposites (d_{001}^{final}) is an indication of the clay dispersion degree. It is useful for comparison purposes but the quantification of clay dispersion degree must be measured by other techniques such as transmission electron microscopy. We also use the parameter Δd_{001} as an indication of the efficiency of polymer chains to intercalate between the silicate layers. For example, suppose that we analyze two nanocomposites A and B with the same polymer matrix but different nanoclays, prepared by identical conditions without thermal degradation of organo-modifiers. Assume that both nanocomposites have the same d_{001}^{final}, suggesting similar clay dispersion degree, but nanocomposite A has higher Δd_{001}. More polymer chains were intercalated between A silicate layers, probably as a consequence of better polymer/clay compatibility in system A, which could be reflected in improved final properties. In this article we use the Δd_{001} parameter to indirectly compare the silicate surface/polymer chains compatibility in the nanocomposite.

Another important factor is the polarity of the clays. The most hydrophilic clay is CNa+, so it is the best candidate for interacting with the most hydrophilic phase (TPS). On the other hand, alkylammonium ion exchange of C30B and C20A allows the conversion of the platelet clay surface from hydrophilic to hydrophobic and increases the interlayer distance as well, therefore they are expected to interact with the PCL.

All the nanocomposites prepared with modified clays showed higher interlaminar space (d_{001}^{final}) than those with CNa^+ reinforcement. This is an indication of higher dispersion of the reinforcement in the matrix, which is a direct result of increased PCL/clay compatibility.[12–18] On the other hand, C30B and C20A nanocomposites showed similar d_{001}^{final} values, suggesting similar clay dispersion degree. On contrast, the Δd_{001} values of the C30B nanocomposites were twice those of C20A the nanocomposites, which can be attributed to improved nanoclay surface/polymer compatibility. Increasing the clay content and matrix compatibilization did not significantly change d_{001}^{final} nor Δd_{001} in any case. It can be concluded that grafting maleic anhydride onto PCL was efficient to improve PCL/TPS compatibility but did not modified matrix/nanoclay interaction.

Thermal Properties

The glass transition (*Tg*) of the matrix is a property that influences the mechanical properties of the nanocomposites. DSC tests were performed to study the effect of nanoclay on thermal properties (*Tg* and melting temperature, *Tm*) of the PCL/TPS matrices. Table III shows the mean values of these properties.

For the neat PCL/TPS and PCL/PCL-gMA/TPS, the *Tg* of PCL was located at −58 °C and −59 °C ± 0.5%, respectively. The incorporation of clay did not significantly change the *Tg* of the matrices. The same result was obtained with the melting temperature of PCL inside the blends which was located between 59 °C and 62 °C ± 0.3% for all samples. Lepoittevin *et al.*[19]

Table III. Effect of Clay Content on the Glass Transition and Melting Temperature of Neat Matrices and Their Nanocomposites

Sample	*Tg* (°C)	*Tm* (°C)	Sample	*Tg* (°C)	*Tm* (°C)
75/0/25/0	−58	59	70/5/25/0	−59	60
75/0/25/1CNa+	−58	60	70/5/25/1CNa+	−56	61
75/0/25/3CNa+	−55	61	70/5/25/3CNa+	−53	61
75/0/25/1C30B	−58	62	70/5/25/1C30B	−54	60
75/0/25/3C30B	−58	60	70/5/25/3C30B	−58	60
75/0/25/1C20A	−57	60	70/5/25/1C20A	−57	61
75/0/25/3C20A	−57	60	70/5/25/3C20A	−54	60

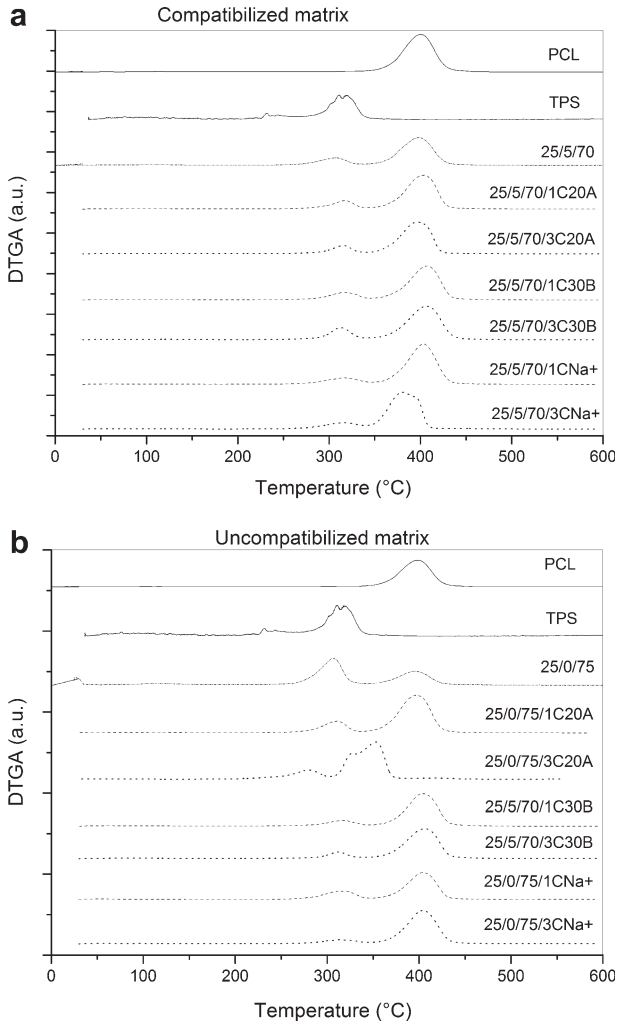

Figure 2. Derivative thermogravimetric analysis of the pure components, neat matrices and nanocomposites: (a) compatibilized matrix; and (b) uncompatibilized matrix.

obtained similar trends for PCL/clay nanocomposites. Melting and glass transition events of TPS, which is the minor component of the blends, could not be recognized by DSC.

Figure 2(a,b) show the DTGA curves of the pure components, neat matrices, and nanocomposites.

Two peaks are observed, the first one at lower temperatures is associated with the degradation of TPS and the degradation nanoclays organo-modifiers that occur at the same range. The second peak corresponds to the PCL degradation. Table IV shows the mean temperature of each degradation step and the mean clay content obtained from DTGA and TGA curves, respectively. Standard deviations below 0.2% were found in all cases.

The clay content inside the nanocomposites was calculated from the residual mass of the nanocomposites at 900 °C correcting for the residual mass of the neat matrices and for the weight loss of the neat clays at the same temperature. The weight loss of the neat clays at 900 °C is mainly composed of water and/or organic content. These calculations were carried out assuming that thermal degradation of the clay organo-modifiers did not take place during the intercalation process. Table IV shows that in all cases the real content of clay inside the nanocomposites is lower than the amount incorporated during processing. Differences up to 23% and 28% were found comparing the clay contents of less and more concentrated systems, respectively. In our case, several parameters act simultaneously (clay content, silicate platelet content, polymer/clay compatibility, clay dispersion degree) and it is not possible to exactly quantify which one dominates each property of the nanocomposites. So, the differences between the real clay content and that used for the preparation of the nanocomposites will not influence the analysis of the final properties. For this reason, we will proceed to use the values of clay content incorporated during processing for each material instead of the real ones in order to clearly identify low and high clay content systems for the analysis of the final properties of the nanocomposites. On the other hand, it can be seen that the addition of clay nor the TPS/PCL compatibilization did significantly change the thermal stability of the pure TPS and PCL components. Even when the PCL/TPS compatibilization was effective, phase separation between these components is still present.[6] Therefore, shifting the temperatures of maximum degradation rates of the pure components is not expected in the blends.

Water Absorption

Figure 3(a,b) show the water uptake of the samples as a function of square root of time.

Table IV. Temperature of Each Degradation Step and the Clay Content Obtained from TGA and DTGA Curves for all Studied Materials Before Biodegradation

Sample	$T1^a$ (°C)	$T2^b$ (°C)	CC^c (wt %)	Sample	$T1^a$ (°C)	$T2^b$ (°C)	CC^c (wt %)
75/0/25/0	298	393	-	70/5/25/0	302	393	-
75/0/25/1CNa+	296	391	0.87	70/5/25/1CNa+	299	391	0.88
75/0/25/3CNa+	302	391	2.34	70/5/25/3CNa+	295	392	2.44
75/0/25/1C30B	302	394	0.76	70/5/25/1C30B	300	390	0.77
75/0/25/3C30B	297	392	2.05	70/5/25/3C30B	300	391	1.88
75/0/25/1C20A	303	391	0.69	70/5/25/1C20A	302	391	0.63
75/0/25/3C20A	301	370	2.16	70/5/25/3C20A	301	385	1.93

[a] $T1$ = Temperature first peak.
[b] $T2$ = Temperature second peak.
[c] CC = Clay content.

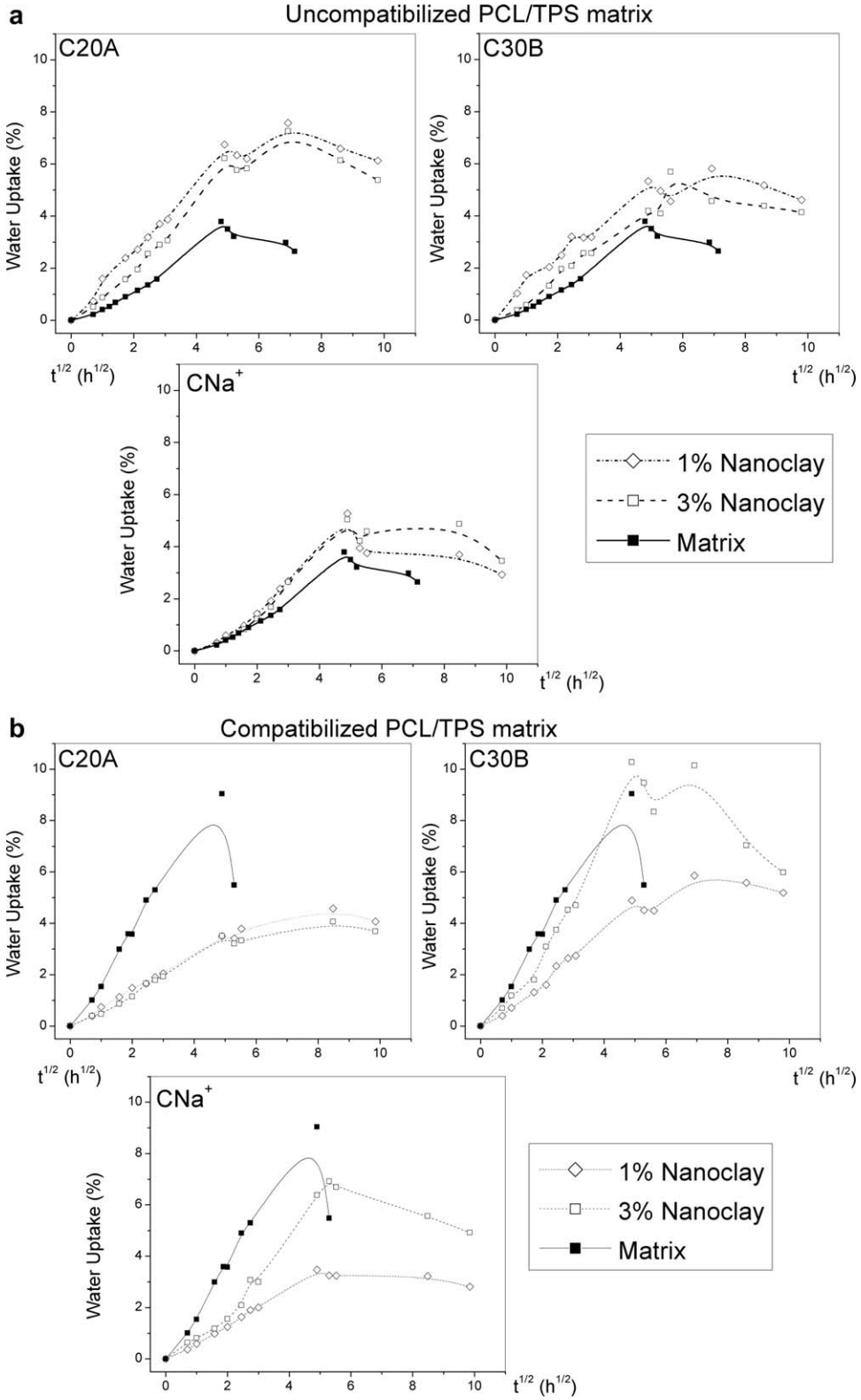

Figure 3. Water uptake as a function of square root of time for the nanocomposites: (a) compatibilized matrix; and (b) uncompatibilized matrix.

The compatibilized matrix [Figure 3(a)] showed greater water uptake than the pure matrix and uncompatibilized nanocomposites because of the addition of hydrophilic groups. The addition of clay was found to reduce water absorption in compatibilized samples, with the exception of C30B. The clay may be located in the amorphous phase producing a network or intricate path for water diffusion.[20,21] Lower water uptake was also found in the compatibilized samples in comparison

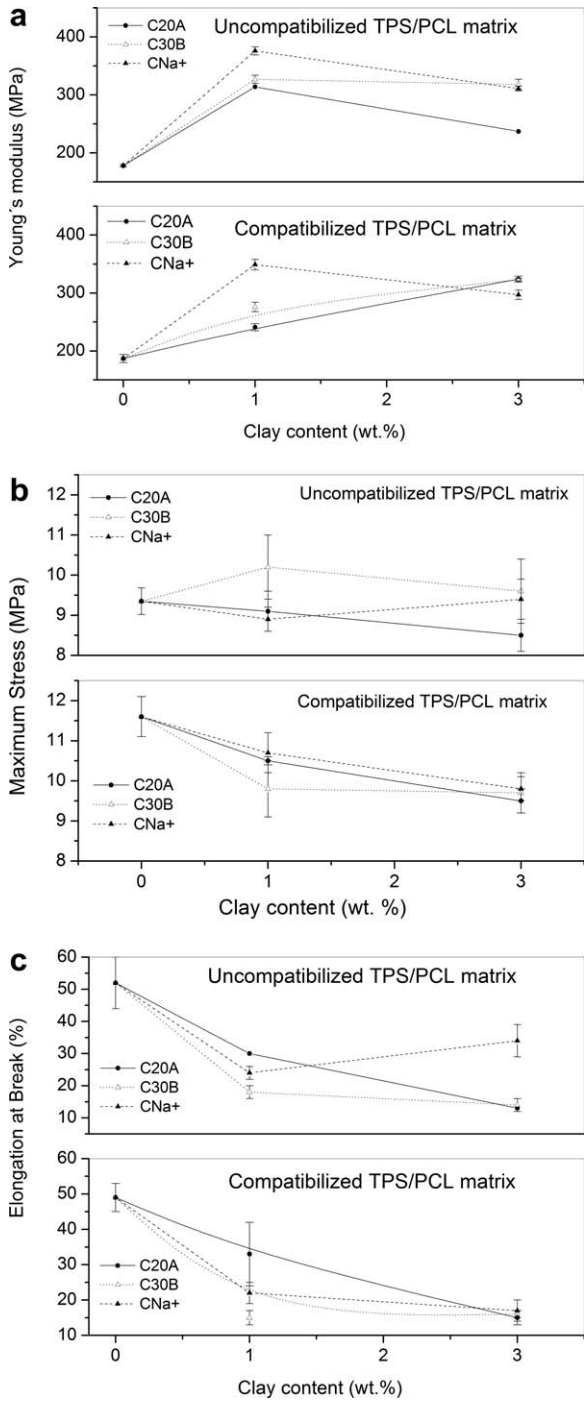

Figure 4. Effect of clay content and matrix compatibilization on the tensile mechanical properties: (a) Youngs modulus, (b) maximum stress, and (c) elongation at break.

with the uncompatibilized ones [Figure 3(b)] for the same clay type and content. The water absorption is mainly because of starch since starch absorbs around 35% of water[22] whereas PCL absorbs around 4% of water.[23] The starch absorption depends on its nature, and if the hydroxyl groups of the starch are interacting with the grafted PCL molecules, the hydrophilic character of the native starch is reduced.[24] In the case of the uncompatibilized specimens, an increase in water absorption after clay incorporation was observed. On the other hand, a clear trend of water absorption as a function of clay modification or clay content was not observed, probably because of TPS dissolution or leaching in the water during the test.[24,25]

Tensile Tests

The mechanical properties of the nanocomposites were evaluated by uniaxial tensile tests. The results are reported in Figure 4(a–c).

PCL is a ductile polymer able to sustain large deformations.[11,12,16,17] The addition of TPS decreased elongation at break and enhanced Youngs modulus and tensile strength.[6] It can be observed in Figure 4(a–c) that all nanoclays increased the Youngs modulus of the TPS/PCL matrix with slight detriments on the maximum stress and elongation at break. Comparing the neat matrices, similar Youngs modulus and higher maximum stress were found for the compatibilized sample. In the case of the nanocomposites the same tendency was observed, similar Youngs modulus and slightly higher maximum stress were obtained for those based on the compatibilized matrix in comparison with the uncompatibilized one. It was shown by XRD that the morphology of the nanocomposites was neither dependent on matrix compatibilization nor on clay content. So, this result is a consequence of the mechanical properties trends after PCL/TPS compatibilization. Regarding nanoclay functionalization, enhanced mechanical properties were found for the C30B nanocomposites in comparison with C20A ones. This result is in accordance with the clay dispersion degree and intercalation efficiency analyzed by XRD. On contrast, CNa+ nanocomposites at low nanoclay content showed the highest Youngs modulus, which was not expected from the morphology analysis. Three parameters will control the final mechanical properties of these materials: nanoclay dispersion degree, silicate surface/polymer compatibility, and silicate content. In the case of the CNa+ nanocomposites, lower clay dispersion degree was found by means of the d_{001}^{final} parameter (XRD), so weaker mechanical properties are expected if only this parameter is analyzed. The compatibility between the polymer blends and nanoclays can be globally and indirectly analyzed in terms of the intercalation efficiency parameter Δd_{001} proposed in this article. The values found for this parameter suggest lower and similar compatibility for CNa+ nanocomposites in comparison with C30B and C20A ones, respectively. Same trend would be expected for mechanical properties if only Δd_{001} is taken into account in the analysis. Finally, clay content is the last factor to be analyzed. All materials were prepared with 1 and 3wt % of each nanoclay. If we think about a phase separated nanocomposite system with CNa+ nanoclay intercalated preferably in the TPS phase (the minor component of the matrix) while C20A and C30B in the PCL one, the TPS phase will have a higher concentration of clay and higher reinforcing efficiency for the same clay dispersion degree. In addition, the reinforcing element of the nanoclay is the silicate platelet. The organo-modified clays are composed by silicate platelets and organic-compounds. The organic content of C30B and C20A is 28 and 40 wt %, respectively (see Table I) while the natural montmorillonite is mainly composed by silicate platelets. So, stronger mechanical properties are expected for CNa+ nanocmposites if only the content of silicate platelets is analyzed. In

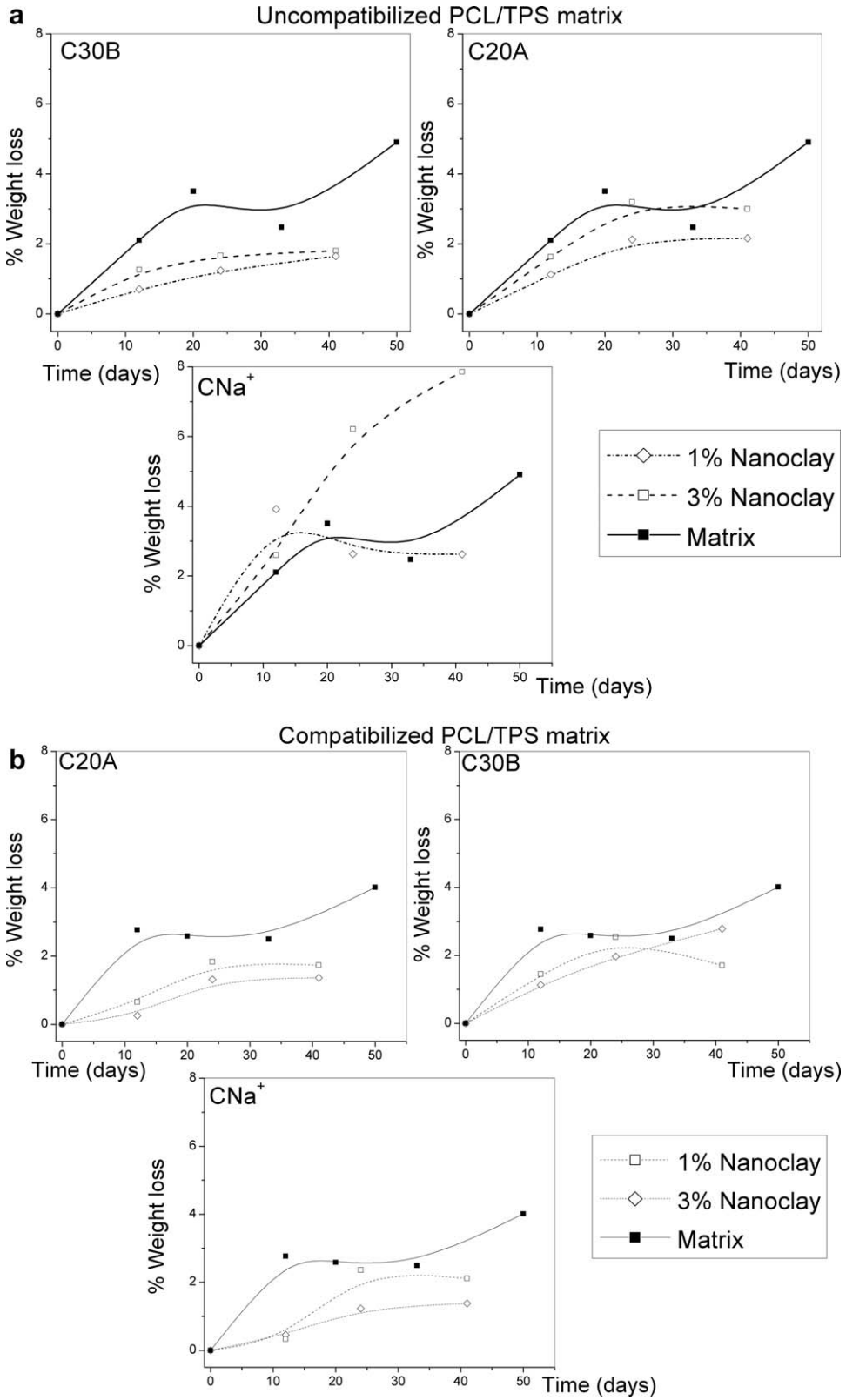

Figure 5. Effect of clay content on the biodegradation behavior of the nanocomposites: (a) compatibilized matrix; and (b) uncompatibilized matrix.

conclusion, in this article, the content of silicate platelets is being the main parameter governing the mechanical properties over the clay dispersion degree and polymer/clay compatibility. Wrong conclusions can be arisen if only clay dispersion degree is analyzed as the dominant parameter governing the mechanical properties of such complex nanocomposite systems.

Table V. Absorbed Water and TPS Loss after 40 Days of Biodegradation in Soil

Sample	W_{eq} (%)	W_{eqsoil}* (%)	TPS loss[a] (%)	Sample	W_{eq} (%)	W_{eqsoil}[a] (%)	TPS loss[a] (%)
75/0/25/0	4	21	-	70/5/25/0	9	8	-
75/0/25/1CNa+	5	15	59	70/5/25/1CNa+	5	9	-
75/0/25/3CNa+	5	20	35	70/5/25/3CNa+	7	15	70
75/0/25/1C30B	6	20	29	70/5/25/1C30B	6	13	-
75/0/25/3C30B	6	13	29	70/5/25/3C30B	10	19	40
75/0/25/1C20A	8	10	-	70/5/25/1C20A	5	9	30
75/0/25/3C20A	7	19	-	70/5/25/3C20A	4	10	38

[a] Calculated after 40 days of biodegradation in soil.

Elongation at break also decreased as a function of clay content independently of the matrix and clay type. Rigid nanoparticles such as clays well dispersed within the matrix may be immobilizing the polymer chains decreasing the polymer ductility.[12]

Biodegradation Tests

Weight loss of the samples as a function of biodegradation time is shown in Figure 5(a,b).

It was observed a slight decrease in the biodegradation rate with the addition of nanoclay. An exception is the case of CNa^+ clay inside the compatibilized blend [Figure 5(a)]. All samples with 3 wt % of clay showed highest biodegradation rate compared to the samples with 1 wt % content. The presence of PCL-gMA did not showed substantial effects in this phenomenon. Similar tendency was found by Fukushima *et al.*[26] who observed that the incorporation of C30B slows the rate of degradation of the polymer attributing this fact to the presence of the reinforcement that can hinder the access of the microorganisms to attack the ester groups of PCL. On contrast, Wu *et al.*[27] have found that the presence of unmodified montmorillonite nanoparticles delay the biodegradation process in composting of the PCL and more as a function of filler content. On the other hand, Singh *et al.*[28] studied the biodegradability of pure PCL and its nanocomposites with two organo-modified clays including Cloisite C30B under controlled conditions in enzyme, pure microorganism (fungi), compost, and Ganges water, finding that the rate of biodegradation dramatically increases by clay incorporation as a result of varying crystallinity and depolymerase activity at different pH arising out of clay incorporation in the matrix. In the case of TPS, Heydari *et al.*[29] found that increasing in CNa+ content decreased biodegradability; while the presence of glycerol, increased it. They explain that increasing in clay content made the polymer surface more hydrophobic, so penetration of water and/or enzymes produced by microorganisms could be reduced, while glycerol should be producing the opposite effect. Shayan *et al.*[30] found that nanoclay slightly increased the amount of biodegradation of polylactic acid/TPS blends that could be because of Aluminum Lewis acid sites of the nanoclay which catalyze the hydrolysis process. Also, the presence of nanoparticles increased the polarity of the substrate and water absorption which increased the heterogenic hydrolysis degradation.

The findings and conclusions of all these works are subject to precise experimental data and they are consistent with the stages of the degradation process of the polymers studied but they show dissimilar tendencies about the effect of polymer/clay nanocomposite parameters such as clay content, polymer/clay compatibility, and clay dispersion degree. In our case, more experimental work is needed to deeply understand the biodegradation process of the systems studied.

Deeper analysis of the biodegradation process was performed calculating the composition of the blends before and after 40 days of biodegradation in soil by TGA. Before testing, the samples were dried in a vacuum oven at 35 °C for 48 h. TPS content was calculated from the mass loss between 175 °C and 375 °C, which is the range of thermal degradation temperatures of ethylenglycol and native starch.[10] PCL content was calculated from the mass loss between 375 °C and 475 °C. Using this information, TPS loss after 40 days of biodegradation in soil was calculated and reported in Table V. In addition, the water absorption of the samples after 40 days of biodegradation in soil (W_{eqsoil}) was calculated as the difference between the wet mass and dried mass of the samples after 40 days of biodegradation in soil. The results are also reported in Table V. Standard deviations for these measurements were below 0.3% for all materials. In previous works[25] we found that 70 wt % of neat TPS is biodegraded after 7 days of biodegradation in soil. In this article, the TPS loss after 40 days of biodegradation was in the range of 30–70% depending of the type of nanoclay in the blend. TPS biodegradation was faster and equilibrium water adsorption was higher after 40 days of biodegradation for the CNa+ based nanocomposites.

CONCLUSIONS

PCL/TPS/nanoclay blends were prepared by melt blending at 110 °C using intensive mixing. Two matrices were used: PCL/TPS compatibilized and PCL/TPS uncompatibilized. Three types of nanoclays were used: two organo-modified montmorillonites with a quaternary ammonium salt (C20A and C30B) and a natural montmorillonite. The effect of clay content was analyzed. An intercalated structure was observed by XRD for all the nanoclays inside the matrices. The nanocomposites prepared with modified clays showed higher clay dispersion degree than those with natural montmorillonite. A parameter for intercalation efficiency calculated by XRD was proposed to indirectly

compare the polymer/clay compatibility. Higher values of this parameter were found for the C30B nanocomposites, suggesting enhanced silicate surface/polymer compatibility. Increasing the clay content and matrix compatibilization did not significantly change clay dispersion neither degree nor intercalation efficiency. So, grafting maleic anhydride onto PCL was efficient to improve PCL/TPS compatibility but did not modified matrix/nanoclay interaction. Glass transition and melting temperatures of the matrices were not significantly changed by clay incorporation. Neither the addition of clay nor the TPS/PCL compatibilization did significantly change the thermal stability of the pure TPS and PCL components calculated by TGA. Regarding water absorption, matrix compatibilization promoted greater water uptake than the uncompatibilized matrix and nanocomposites because of the addition of hydrophilic groups. On the other hand, a clear trend of water absorption as a function of clay modification or clay content was not observed, which was attributed to TPS dissolution or leaching in the water during the test. On the other hand, it was observed a slight decrease in the biodegradation rate by the addition of nanoclay, except to natural montmorillonite. Matrix compatibilization and nanoclays increased the Youngs modulus of the TPS/PCL matrix. The optimal case was obtained with the 1 wt % CNa+ nanocomposites increasing 101% the Youngs modulus with slight detriments of the maximum tensile stress and elongation at break. In contrast with the expected results, this nanocomposite showed the lowest clay dispersion degree and intercalation efficiency in the blends. It is concluded that the mechanical properties are governed by three parameters that act simultaneously: nanoclay dispersion degree, nanoclay layer surface/polymer compatibility and silicate platelet content. The improved mechanical properties observed for the CNa+ nanocomposites can be a consequence of the silicate platelet content acting as the dominant parameter.

ACKNOWLEDGMENTS

This article was supported by the National Agency of Science and Technology (ANPCyT) [Fonarsec FSNano004]; and the National University of Mar del Plata (UNMdP) [15G327].

REFERENCES

1. Shen, Z. Q.; Hu, J.; Wang, J. L.; Zhou, X. Y. *J. Int. J. Environ. Sci. Technol.* **2015**, *12*, 1235.
2. López, O. V.; Ninago, M. D.; Lencina, M. M. S.; García, M. A.; Andreucetti, N. A.; Ciolino, A. E.; Villar, M. A. *Carbohydr. Polym.* **2015**, *126*, 83.
3. Wu, C. S. *Polym. Degrad. Stab.* **2003**, *80*, 127.
4. Kalambur, S. S. H. Rizvi, *J. App. Polym. Sci.* **2005**, *96*, 1072.
5. Reddy, M.; Vivekanandhan, S.; Misra, M.; Bhatia, S.; Mohanty, A. *Prog. Polym. Sci.* **2013**, *38*, 1653.
6. Guarás, M. P.; Alvarez, V. A.; Ludueña, L. N. *J. Polym. Res.* **2015**, *22*, 165.
7. Romero-Bastida, C. A.; Bello-Pérez, L. A.; Velazquez, G.; Alvarez-Ramirez, J. *Carbohydr. Polym.* **2015**, *127*, 195.
8. Avella, M.; De Vlieger, J. J.; Errico, M. E.; Fischer, S.; Vacca, P.; Volpe, M. G. *Food Chem.* **2005**, *93*, 467.
9. Rhim, J. W.; Park, H. M.; Ha, C. S. *Prog. Polym. Sci.* **2013**, *38*, 1629.
10. Yahiaoui, F.; Benhacine, F.; Ferfera-Harrar, H.; Habi, A.; Hadj-Hamou, A. S.; Grohens, Y. *Polym. Bull.* **2015**, *72*, 235.
11. Ludueña, L. N.; Kenny, J. M.; Vázquez, A.; Alvarez, V. A. *Mater. Sci. Eng. A Struct.* **2011**, *529*, 215.
12. Ludueña, L.; Alvarez, V.; Vázquez, A. *Mater. Sci. Eng. A Struct.* **2007**, *460–461*, 121.
13. Cui, Y.; Kumar, S.; Rao Konac, B.; van Houcke, D. *RSC Adv.* **2015**, *5*, 63669.
14. Kotal, M.; Bhowmick, A. K. *Prog. Polym. Sci.* **2015**, *51*, 127. 1.
15. Di Maio, L.; Garofalo, E.; Scarfato, P. *Polym. Compos.* **2015**, *36*, 1135.
16. Ludueña, L. N.; Vazquez, A.; Alvarez, V. A. *J. Compos. Mater.* **2012**, *46*, 677.
17. Ludueña, L. N.; Vazquez, A.; Alvarez, V. A. *J. Appl. Polym. Sci.* **2013**, *128*, 2648.
18. Ludueña, L.; Kenny, J.; Vázquez, A.; Alvarez, V. *J. Compos. Mater.* **2014**, *48*, 2059.
19. Lepoittevin, B.; Devalckenaere, M.; Pantoustier, N. *Polymer* **2002**, *43*, 4017.
20. Liu, X.; Wu, Q.; Berglund, L. A.; Fan, J.; Qi, Z. *Polymer* **2001**, *42*, 8235.
21. Pérez, C. J.; Alvarez, V. A.; Stefani, P. M.; Vázquez, A. *J. Therm. Anal. Calorim.* **2007**, *88*, 825.
22. Pandey, J.; Singh, R. *Starch/Starke* **2005**, *57*, 8.
23. Gaspar, M.; Benk, Z.; Dogossy, G.; Reczey, K.; Czigany, T. *Polym. Degrad. Stabil.* **2005**, *90*, 563.
24. Pang, M.; Pun, M.; Mohd, I. Z. A. *J. Appl. Polym. Sci.* **2013**, *129*, 3656.
25. Berruezo, M.; Ludueña, L. N.; Rodriguez, E.; Alvarez, V. A. *J. Plast. Film. Sheet* **2014**, *30*, 141.
26. Fukushima, K.; Abbate, C.; Tabuani, D.; Gennari, M.; Rizzarelli, P.; Camino, G. *Mater. Sci. Eng. C* **2010**, *30*, 566.
27. Wu, T.; Xie, T.; Yang, G. *Appl. Clay Sci.* **2009**, *45*, 105.
28. Singh, N. K.; Purkayastha, B. D.; Roy, J. K.; Banik, R. M.; Yashpal, M.; Singh, G.; Malik, S.; Maiti, P. *ACS Appl. Mater. Interfaces* **2010**, *2*, 69.
29. Heydari, A.; Alemzadeh, I.; Vossoughi, M. *IJE Trans. B Appl.* **2014**, *27*, 203.
30. Shayan, M.; Azizi, H.; Ghasemi, I.; Karrabi, M. *Carbohydr. Polym.* **2015**, *124*, 237.